

# Comparing different recalibrated methods for estimating mean radiant temperature in outdoor environment

Wanlu Ouyang <sup>a</sup>, Zhixin Liu <sup>a,\*</sup>, Kevin Lau <sup>b</sup>, Yuan Shi <sup>c</sup>, Edward Ng <sup>a,d,e</sup>

<sup>a</sup> School of Architecture, The Chinese University of Hong Kong, New Territories, Hong Kong, China

<sup>b</sup> Department of Civil, Environmental and Natural Resources, Luleå Tekniska Universitet, Sweden

<sup>c</sup> Department of Geography & Planning, University of Liverpool, Liverpool, UK

<sup>d</sup> Institute of Future Cities, The Chinese University of Hong Kong, New Territories, Hong Kong, China

<sup>e</sup> Institute of Environment, Energy and Sustainability, The Chinese University of Hong Kong, New Territories, Hong Kong, China

\*Corresponding author: E-mail address: [zhixinliu@cuhk.edu.hk](mailto:zhixinliu@cuhk.edu.hk) (Z. Liu)

## Abstract:

Mean radiant temperature (MRT) is a significant variable for outdoor thermal comfort studies. Two measurement-based methods can estimate MRT, one is globe thermometer – cheap, easily-applied but inaccurate, another is integral radiation measurement method (also known as the six-directional method) - accurate but expensive. Due to low-cost and convenience, the globe thermometer has been widely used. Previous studies have improved its estimation accuracy by recalibrating the convection coefficients in the ISO conventional equation. Thus, it is pending to cross-compare the performance of these recalibrated methods.

This study aims to investigate the transferability of the recalibrated methods for estimating MRT in outdoor environment. First, field measurement was conducted in a subtropical city, Hong Kong. MRT was obtained through two methods: globe thermometer and integral radiation method. Second, the existing recalibrated convection coefficients were summarized, and the localized convection coefficient was recalibrated. Third, all recalibrated methods were compared for their performance. The impacts of measurement locations, devices, analysis time intervals were examined.

The results showed that the newly recalibrated method achieved the lowest estimation errors (RMSE = 3.84 °C). Other recalibrated methods presented higher RMSE (3.84 – 17.52 °C), similar as conventional ISO method (7.91 °C). Especially for open spaces, the coefficients from other cities should be cautiously applied when the accuracy requirement is less than  $\pm 2$  °C. Kestrel and Grey globe are more recommended in subtropical cities. This study shed light on the application of globe thermometer for outdoor environment, and emphasized the necessity in recalibrating the convection coefficients locally.

## Keywords:

Mean radiant temperature, outdoor thermal comfort, field measurement, globe thermometer, Integral radiation measurement (IRM), convection coefficient

## Nomenclature

---

MRT	Mean radiant temperature (°C)
ISO	International Organization for Standardization
IRM	Integral radiation measurement method
UHI	Urban heat island
$R^2$	The coefficient of determination
d	The index of agreement
MAE	Mean absolute error
MBE	Mean bias error
RMSE	Root mean square error
RMSEs	Systematic root mean square error
RMSEu	Unsystematic root mean square error
$K_i$	Shortwave radiation fluxes ( $\text{Wm}^{-2}$ )
$L_i$	Longwave radiation fluxes ( $\text{Wm}^{-2}$ )
$W_i$	The angular factor for six directions
$\alpha_k$	The absorption coefficients of the clothed human body for shortwave radiations
$\varepsilon_p$	The absorption coefficients of the clothed human body for longwave radiations
$\sigma$	The Stefan-Boltzmann constant ( $= 5.67 \cdot 10^{-8} \text{ Wm}^{-2}$ )
$h_{cg}$	The coefficient of heat transfer by convection of the globe
$V_a$	The wind speed (m/s)
$T_g$	The globe temperature (°C)
$T_a$	The air temperature (°C)
$\varepsilon$	The globe emissivity
$D$	The globe diameter (m)
$T_i$	The MRT value estimated by globe thermometer method (°C)
$S_i$	The MRT value estimated by integral radiation measurement method (°C)
$\bar{S}$	The mean of the MRT value estimated by integral radiation measurement method (°C)
$N$	Number of the data

---

## 1. Introduction

### 1.1. Climate change and human biometeorology

Due to climate change, extreme weather events are increasing and intensifying (IPCC, 2021). Ongoing urbanization processes not only accommodate the ever-increasing population, but also lead to urban heat islands phenomenon (UHIs)(Oke, 1982). Coupling the heatwaves and UHIs, the urban areas are exposed to severe and devastating heat-related mortality and morbidity (D. Wang et al., 2019). Therefore, it is significant to understand the mechanisms of urban climate and identify the measures to better cope with heat stress.

Human biometeorology is a science about the interactions between the human body and atmospheric environment (Höppe, 1997). It involves multiple disciplines related to human heat stress and outdoor thermal comfort, i.e., urban climate, urban planning and design, therefore it is gaining increasing attentions in the context of urban heat islands and global warming (McGregor, 2012). There are two main aspects to quantify the human thermal environment: one aspect is human body characteristics – the clothing insulation, the metabolic rate, and human body parameters (age, gender, height, weight); another perspective is meteorological variables - air temperature, air velocity, humidity, and mean radiant temperature (Kántor et al., 2015).

### 1.2. Mean radiant temperature and measurement-based technologies for its estimation

Mean radiant temperature (MRT) is a key variable for outdoor thermal comfort, as it is decisive for the energy balance of the human body. Defined as “the uniform temperature of an imaginary enclosure in which radiant heat transfer from the human body equals the radiant heat transfer in the actual non-uniform enclosure” (ASHRAE, 2001), the concept of MRT enables the investigations in the radiative exchange between human body and its surrounding environment (ISO, 2001). MRT has been widely used and assessed in outdoor thermal comfort and climate-sensitive studies, i.e., calculating the outdoor thermal comfort index (Guo et al., 2020), predicting heat-related mortality (Thorsson et al., 2014), investigating the effect of urban geometry for heat stress (Lau et al., 2015).

Currently, there are two main measurement-based methods to estimate MRT, one is the integral radiation measurement method (IRM) and another is globe thermometer. IRM is deemed as the most accurate method to obtain MRT estimations (Thorsson et al., 2007), which uses pyranometer to measure the shortwave radiative fluxes and pyrgeometer to collect the longwave radiative fluxes. Afterwards, the six-directional short- and long-wave radiations are integrated with different factors following the equation (1) – (2) (Kántor & Unger, 2011; Thorsson et al., 2007). Albeit the high accuracy, this method is with high costs and complexity so that is not as common as the globe thermometer method (Lee et al., 2021; Thorsson et al., 2007). Globe thermometer is one of the most popular instruments in urban climate studies for MRT estimation (Johansson et al., 2014). It is based on an assumption that the radiant heat transfer depends on the surface temperature of the globe, and the convection can be estimated by air temperature and wind speed as proxies (ISO, 2001). The standard globe thermometer has a diameter of 0.15m, and is proposed for indoor environment originally. Then MRT can be estimated based on globe temperature following the equation (3) – (4) (ISO, 2001).

$$S_{str} = \alpha_k \sum_{i=1}^6 W_i K_i + \varepsilon_p \sum_{i=1}^6 W_i L_i \quad (1)$$

$$MRT = \sqrt[4]{S_{str}/(\varepsilon_p \sigma)} - 273.15 \quad (2)$$

$$h_{cg} = 1.1 \times 10^8 V_a^{0.6} / D^{0.4} \quad (3)$$

$$MRT = \left[ (T_g + 273.15)^4 + \frac{h_{cg}}{\varepsilon} \times (T_g - T_a) \right]^{0.25} - 273.15 \quad (4)$$

Where  $K_i$  is the shortwave radiation fluxes ( $i = 1 - 6$ );  $L_i$  is the longwave radiation fluxes ( $i = 1 - 6$ );  $W_i$  is the angular factor for six directions with the sum weightings as 1, value as 0.22 for the lateral directions, and 0.06 for the up-down directions;  $\alpha_k$  and  $\varepsilon_p$  are the absorption coefficients of the clothed human body for shortwave and longwave radiations, equal 0.7 and 0.97 respectively;  $\sigma$  is the Stefan-Boltzmann constant as  $5.67 \times 10^{-8} \text{ Wm}^{-2}$ ;  $h_{cg}$  is the coefficient of heat transfer by convection of the globe;  $V_a$  is the wind speed (m/s);  $T_g$  is the globe temperature ( $^{\circ}\text{C}$ );  $T_a$  is the air temperature ( $^{\circ}\text{C}$ );  $\varepsilon$  is the globe emissivity, as 0.95 for the black globe;  $D$  is the globe diameter (unit should be m!).

### 1.3. Recalibration for globe thermometer

Although the globe thermometer is popular for MRT estimation, it is still questionable to be used in outdoor environments with potentially rapid changing radiant and wind conditions (Teitelbaum et al., 2020). Three main reasons can explain the unsuitability (Kántor et al., 2015): 1) the standard globe usually takes over 20min to reach the equilibrium, which is too long for the outdoor environment with rapidly changing microclimate variables, i.e., air velocity and radiations. Therefore, the equilibrium status may not be achieved and the accuracy of the MRT estimation is uncertain; 2) the black color of the globe may absorb the shortwave radiation than expected, but it assumes both longwave and shortwave radiations are absorbed equally in the calculation of the globe thermometer; 3) the shape of the globe can be a good approximation for the seated human body, but not representative for a standing person. The spherical globe averages the radiation from all directions equally, thus may bring some estimation deviations.

Given the limitations illustrated above, some studies reduced the size of the globe to 30-50mm, which was proved to effectively shorten the equilibrium time within 5min (Nikolopoulou et al., 1999; Thorsson et al., 2007). Besides, the grey color globe was suggested to be used, as the light color is closer to the radiant properties of the skin and clothing of human beings (Kántor & Unger, 2011). As the convection coefficient  $h_{cg}$  in conventional method following the equation (3) is developed for the black globe with 150mm diameter in indoor environment. For outdoor environment, the mean convection coefficients should be recalibrated for the global thermometer with smaller size and different color (Vanos et al., 2021; S. Wang & Li, 2015).

Some researchers have recalibrated the convection coefficients of the globe thermometer for the outdoor environment in different climate backgrounds, i.e., temperate oceanic climate ( $Cfb$ ) in Gothenburg, Sweden (Thorsson et al., 2007), tropical rainforest climate ( $Af$ ) in Singapore (Acero et al., 2021; C. L. Tan et al., 2013, 2015), humid subtropical climate ( $Cwa$ ) in Chandigarh, India (Manavvi & Rajasekar, 2020), and hot arid climate ( $Bwh$ ) in Tempe, Arizona (Vanos et al., 2021). These studies used the MRT values estimated by integral radiation measurement as a benchmark, and applied non-linear regression to recalibrate the convection coefficient of the globe thermometer. Since in these studies, the sphere color (i.e., black and grey) and diameter (i.e., 38mm, 40mm, 50mm, 150mm) varied, and the background climates are different, the recalibrated convection coefficients are dissimilar (detailed values are summarized in the **Table 2** in Methodology section).

### 1.4. Research gaps and objective

Based on the above information, three research gaps can be identified: 1) current literature recalibrated the convection coefficients in the local context, it is a pending question whether the recalibrated convection coefficients are transferable to other cities with similar or different climate backgrounds; 2) previous studies usually measure MRT and recalibrate the convection coefficients in open space, whether the coefficients can be used in other urban environments, i.e., the street canyon or tree-shaded area, is scarcely discussed so far; 3) previous studies used different thermometers to obtain  $T_g$ , it is difficult to cross-compare the impacts of the devices on the performance of different recalibrated

methods. Besides, the impacts of the analysis intervals should also be explored, as the outdoor environment is featured with fast varying wind and solar conditions.

Therefore, this study aims to systematically compare the suitability of existing recalibrated methods for MRT estimation in different built environments. To achieve this aim, field measurement campaigns were firstly conducted in three sites in a subtropical city Hong Kong, i.e., open space, under tree-shading, and street canyon. Thereafter, the convection coefficient was recalibrated locally for Hong Kong. Thirdly, the MRT values were calculated based on the recalibrated methods in the previous studies and this study, and the strengths and limitations of them were assessed and compared. Besides, the impacts of measurement locations, device types, and analysis time intervals were explored and compared.

## 2. Methodology

The framework of the methodology in this study is presented in **Fig. 1**, including three steps: field measurement, recalibrated methods, and performance comparison of the previous recalibrated and localized recalibrated methods.

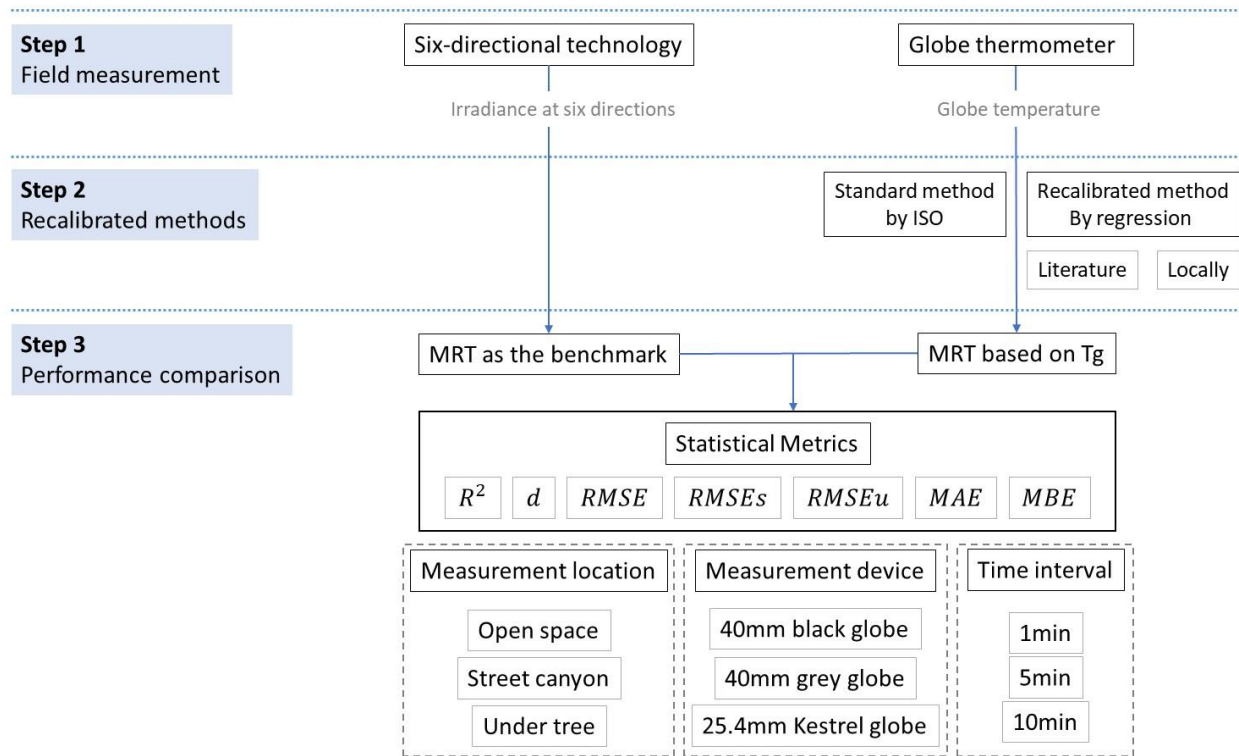


**Fig.1.** Flowchart of the methodology in this study

### 2.1. Study area

Hong Kong (HK) is located on the eastern Pearl River Delta in South China, which is featured with a humid subtropical climate (*Cfa* based on Köppen climate classification). Experiencing a long and hot summer from June to September, HK has a daily mean value of air temperature at 28.4 ~ 30.2 °C, relative humidity at 73 ~ 84 %, and direct solar radiation at 6.08 ~ 16.33 MJ/m<sup>2</sup> during 2019-2020 (HKO, 2019, 2020). The three measurement sites are located in the Chinese University of Hong Kong, including open space at the rooftop, street canyon between two rows of buildings in the north-south orientation, and under tree-shading near to an artificial lake. The surrounding environment of the sites and their sky view factor (SVF) were shown in **Fig. 2**.

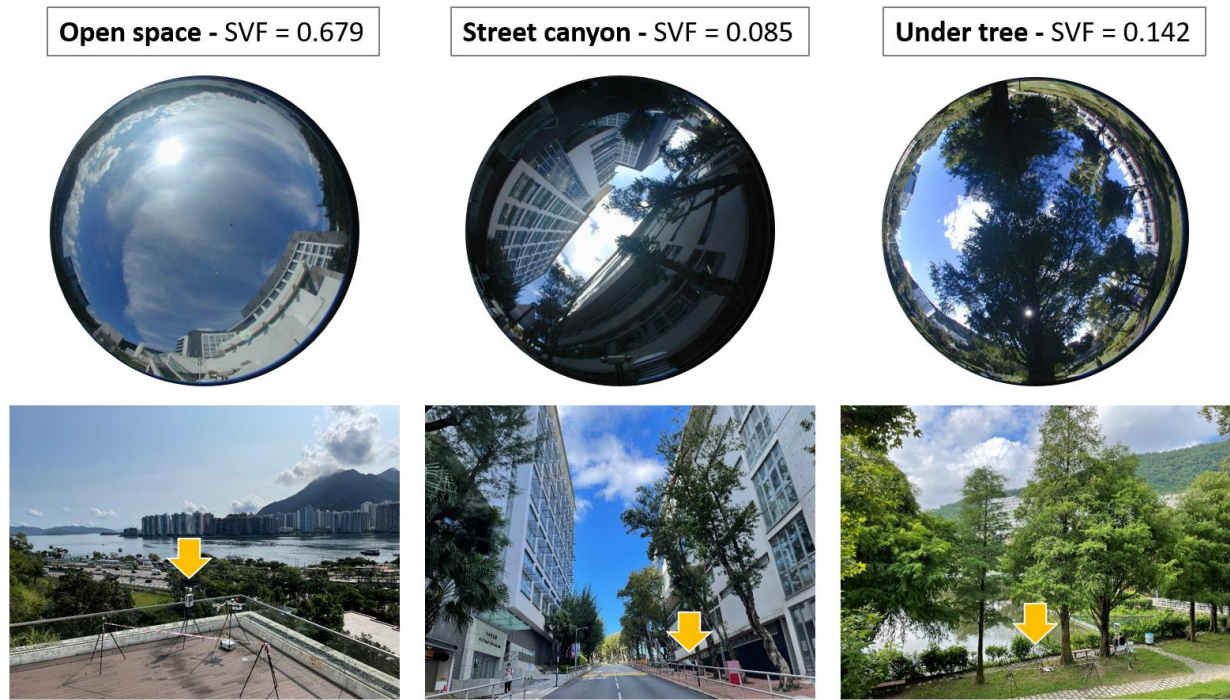


**Fig. 2.** Measurement sites and SVF

## 2.2. Measurement scheme

The measurement campaign was taken in six partially cloudy days totally, two days for each site: Sep. 6<sup>th</sup> and Sep. 10<sup>th</sup> for the open space site, Sep. 2<sup>th</sup> and Sep. 9<sup>th</sup> for the street canyon site, Aug. 30<sup>th</sup> and Sep. 3<sup>rd</sup> for under tree site. On each day, the microclimate variables were collected simultaneously by stationary measurement from 9:00-17:00 (local time). Air temperature, relative humidity, wind speed, 40mm black global temperature and 40mm grey global temperature were measured by TESTO480, while 25.4mm black global temperature was collected by Kestrel 5400. Besides, two sets of equipment were used to record six-directional radiations – Apogee by Apogee Instruments and CNR4 by Kipp & Zonen. All devices were set on the pedestrian height at around 1.5m. The instrument specifications can be found in **Table 1**. It should be noteworthy that the globe temperature measured by the Kestrel is converted to the equivalent temperature for a standard globe, thus the diameter of Kestrel globe should be 150mm in the calculation (Kestrel Instruments, 2021).

**Table 1.** Equipment specifications

Sensors	Variable(s)	Range	Accuracy	Sampling
Testo 480 Comfort level probe	Wind speed	0 to 5 m/s	$\pm 0.03$ m/s + 4% of mv	1 min
Testo 480 Temperature probe	Air temperature Relative humidity	-20 to +70 °C 0 to 100 %	$\pm 0.2$ °C $\pm 1\%$	1 min
Testo 480 Global thermometer 40mm	Global temperature	0 to 120 °C	Class 2*	1 min
Kestrel 5400 Heat stress tracker 1 inch	Global temperature	-29.0 to 60.0 °C	1.4 °C	1 min
CNR4 Component net radiometers	Longwave and shortwave radiation in six directions	-250 to +250 W/m <sup>2</sup> (net longwave irradiance) 0 to 2000 W m <sup>-2</sup> (net shortwave irradiance)	<b>Pyrgometer:</b> 5 to 15 $\mu$ V/W/m <sup>2</sup> <b>Pyranometer:</b> 10 to 20 $\mu$ V/W/m <sup>2</sup>	1 min
Apogee four- component net radiometer	Longwave and shortwave and radiation in six directions	-200 to 200 W m <sup>-2</sup> (net longwave irradiance) 0 to 2000 W m <sup>-2</sup> (net shortwave irradiance)	<b>Pyrgometer:</b> 0.12 mV per W m <sup>-2</sup> <b>Pyranometer:</b> 0.057 mV per W m <sup>-2</sup> (upward-looking); 0.15 mV per W m <sup>-2</sup> (downward-looking)	1 min

\*According to standard EN 60584-2, the accuracy of Class 2 to -40 to +1200 °C (Type K)

### 2.3. The recalibrated methods

Current literature have recalibrated the heat convection coefficients based on the non-linear regression analysis. Using MRT values measured by integral radiation measurement as a benchmark, the best curve fit is obtained based on a higher coefficient of determination. Summarized in **Table 2**, these studies applied globe spheres with different diameters and colors, and were conducted in various climate backgrounds, thus the coefficients were dissimilar. **Table 2** also provides a new recalibrated convection

coefficient for Hong Kong, which is based on the non-linear regression results for three measurement locations and three globe devices (the details can be found in [Section 3.3](#)). Based on the listed recalibrated coefficients, the corrected values can be calculated with  $T_g$  measured by globe thermometer. Thereafter the performance of the recalibrated methods can be assessed and compared based on the MRT measured by integral radiation measurement.

#### 2.4. The statistical metrics

Based on the recommendation of previous studies (Willmott, 1981, 1982), five metrics were used to illustrate the comparison between different methods: the coefficient of determination ( $R^2$ ), the root mean square error (RMSE), and its two substances - the systematic root mean square error (RMSEs) and the unsystematic root mean square error (RMSEu), the index of agreement (d), the mean bias error (MBE), and the mean absolute error (MAE).  $R^2$  quantifies the variation between paired observations, while d indicates the ratio between the mean square error and the potential error. Both  $R^2$  and d are dimensionless indexes, ranging from 0 to 1. RMSE describes the mean level of errors, substituted of systematic and unsystematic errors. RMSEs represents the errors existing constantly, whereas RMSEu estimates the unsystematically appearing effects. MBE denotes the average differences between paired observations, as positive value indicates overestimation and negative value implicates underestimation. MAE measures the absolute errors between paired observations. When paired observations are more similar,  $R^2$  and d are closer to 1, RMSE and RMSEs closer to 0, RMSEu closer to RMSE, MBE and MAE closer to 0. The formulas to calculate these metrics are listed below:

$$d = 1 - \left[ \frac{\sum_{i=1}^N (T_i - S_i)^2}{\sum_{i=1}^N (|T'_i| + |S'_i|)^2} \right] \quad (5)$$

$$RMSE = \left[ RMSE_s^2 + RMSE_u^2 \right]^{1/2} = \left[ N^{-1} \sum_i^n (T_i - S_i)^2 \right]^{1/2} \quad (6)$$

$$\text{Where: } RMSE_s = \left[ N^{-1} \sum_i^n (\hat{T}_i - S_i)^2 \right]^{1/2} \quad (6a)$$

$$RMSE_u = \left[ N^{-1} \sum_i^n (T_i - \hat{T}_i)^2 \right]^{1/2} \quad (6b)$$

$$MAE = N^{-1} \sum_i^n (|T_i - S_i|) \quad (7)$$

$$MBE = N^{-1} \sum_i^n (T_i - S_i) \quad (8)$$

Where  $T'_i = T_i - \bar{S}$ ,  $S'_i = S_i - \bar{S}$ , and  $\hat{T}_i = a + b * S_i$ ;  $T_i$  is the MRT value estimated by globe thermometer;  $S_i$  represents the MRT value estimated by integral radiation measurement method;  $\bar{S}$  represents the mean of the MRT value estimated by integral radiation measurement method;  $N$  denotes the number of the data;



**Table 2.** Standard and recalibrated methods for MRT estimation

Source	Method name in this study	Globe thermometer	Heat convection coefficient	Limits
ISO 7726 (1998)	ISO	Black globe, 150mm	$h_c = 1.1 * 10^8 * V_a^{0.6} / D^{0.4}$	Not specific
(Thorsson et al., 2007)	Thorsson	Grey globe, 38mm	$h_c = 1.335 * 10^8 * V_a^{0.71} / D^{0.4}$	$0.1 \leq Va \leq 4.0$ $100 \leq SWin \leq 850$
(Tan et al., 2013)	Tan	Grey globe, 40mm	$h_c = 3.42 * 10^8 * V_a^{0.119} / D^{0.4}$	$0 \leq Va \leq 4.0$ $SWin \leq 1300$
(Manavvi & Rajasekar, 2020)	Manavvi	Grey globe, 50mm	$h_c = 1.5 * 10^8 * V_a^{0.93} / D^{0.4}$	$0.1 \leq Va \leq 4.0$ $SWin \leq 950$
(Teitelbaum et al., 2020)	TeitelbaumFree	Black globe, 150mm	$Nu_{free} = 2 + \frac{0.589Ra^{0.25}}{(1 + (0.469/Pr)^{9/16})^{4/9}}$ $Ra = \frac{g\beta}{\nu\alpha} (t_a - t_g) D^3$ $Pr = \frac{c_p\mu}{k}$	Free convection $Pr \geq 0.7$ $Ra \leq 10^4$
	TeitelbaumForce		$Nu_{force} = 2 + (0.4Re^{0.5} + 0.06Re^{2/3})Pr^{0.4}$ $Re = \frac{v_a D}{\nu}$	Forced $0.7 \leq Pr \leq 380$ $0.7 \leq Ra \leq 76000$
	TeitelbaumMix		$Nu_{mixed} = (Nu_{free}^n + Nu_{forced}^n)^{1/n}$	Mixed $n = 4$

			$MRT = \sqrt[4]{(T_g + 273.15)^4 + \frac{Nu * k}{\epsilon \sigma D} * (T_g - T_a) - 273.15}$	
(Vanos et al., 2021)	VanosStandard	Black globe, 150mm	$MRT_{SGT} = \sqrt[4]{(T_s + 273.15)^4 + \frac{1.1 * 10^8 * V_a^{0.6}}{\epsilon * D^{0.4}} * (T_s - T_a) - 273.15}$ $T_s = 1.345 * T_g - 0.369 * T_a + 0.725$	Not specific
	VanosBlack	Black globe, 40mm	$MRT_{SGT} = \sqrt[4]{(T_s + 273.15)^4 + (0.24 + 2.08V_a^{0.5} + 1.14V_a^{0.667}) * 10^8 * (T_s - T_a) - 273.15}$ $T_s = 1.851 * T_g - 0.915 * T_a + 0.404 \text{ for black}$ $T_s = 1.6 * T_g - 0.339 * T_a - 8.69 \text{ for grey}$	Not specific
	VanosGrey	Grey globe, 40mm		
(Acero et al., 2021)	Acero	Black globe, 150mm	$h_c = 0.88 * 10^8 * V_a^{0.46} / D^{0.4}$	Not specific For clear and overcast weather
This study*	HKCorrect	Black globe, 40mm Black globe, 25.4mm (Kestrel) Grey globe, 40mm	$h_c = 0.678 * 10^8 * V_a^{0.019} / D^{0.4}$	$0.23 \leq Va \leq 3.06 \text{ m/s}$ SWdown $\leq 1036 \text{ W/m}^2$

\*The recalibration process and results were reported in the Result section

### 3. Results

#### 3.1. Measurement results

##### 3.1.1. Integral radiation measurement and results

Previous studies usually used the MRT estimated by the integral radiation measurement (IRM) as the benchmark (C. L. Tan et al., 2013; Teitelbaum et al., 2020), as it was identified as the most accurate means to estimate MRT so far (Thorsson et al., 2007). This study applied two instruments based on IRM to estimate the MRT as the benchmark, one is the widely used CNR4 (Acero et al., 2021; Lai et al., 2017; Ouyang et al., 2021; C. L. Tan et al., 2013), another is recently emerging Apogee (Teitelbaum et al., 2020). To compare the different recalibrated methods based on a solid benchmark, the reliability of the IRM was justified in this sub-section.

As shown in **Fig. 3**, MRT measured by CNR4 and Apogee showed a high correlation at 1-min measurement interval, all above 0.88 irrespective of measurement locations. Especially for open space, these two instruments presented nearly similar values, as the correlation coefficients were near to 1 (**Fig. 3-a**), and the differences of them showed random patterns (**Fig. 3-b**). CNR4 estimated slightly higher MRT values than Apogee in the street canyon, and presented slightly lower values under tree. The detailed statistics of MRT estimated by CNR4 and Apogee were shown in **Table 3**. The deviations between these two methods were higher in the locations of open space and street canyon, as RMSE, MAE and MBE were relatively higher than the values of under tree location. One possible reason is the placement of the sensors of two methods cannot be identical, as the equipment was placed nearer to a road and a pedestrian lane for the street canyon location, and is nearer to a glass railing for the open space location (See **Fig. 2**). Therefore, the radiations from the surrounding may vary in the complex environment given the high sensitivity of these two instruments.

Based on the above analysis, MRT estimated by IRM was justified to be the benchmark in this study. And we applied the mean of the values of Apogee and CNR4 in the following analysis as the benchmark, thus some possible deviations related to instrument positions could be removed.

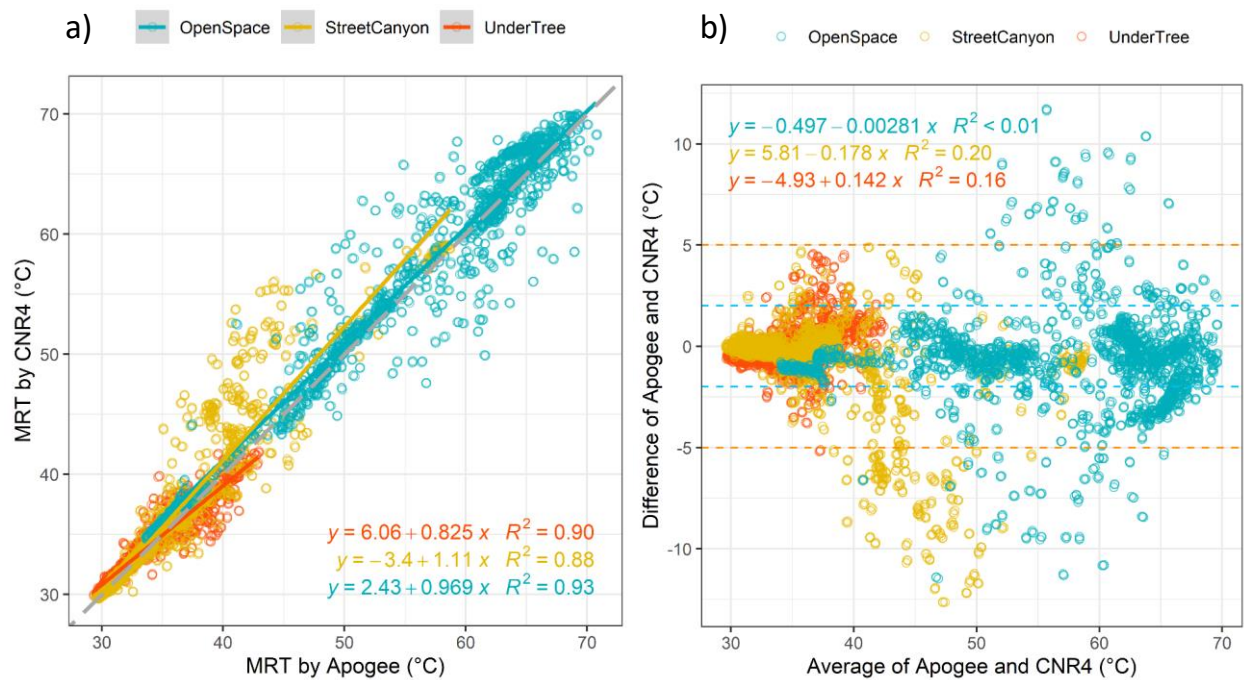


**Fig. 3.** Comparison between MRT by two IRM at 1 min interval: a) correlation between MRT by CNR4 vs. Apogee; b) difference between MRT by CNR4 and Apogee vs. mean values of MRT by two methods.

In a), the grey dash line shows the reference line  $y = x$ ; in b) the blue dash line shows the  $\pm 2$  °C accuracy requirement for comfort class, and the orange dash line shows the  $\pm 5$  °C accuracy requirement for stress class based on ISO standard (ISO, 1985).

**Table 3.** Quantitative metrics of the MRT by CNR4 vs. Apogee at 1-min time interval (unit: °C)

Location	R <sup>2</sup>	d	RMSE	RMSEs	RMSEu	MAE	MBE
Under Tree	0.90	0.97	0.94	0.23	0.92	0.61	-0.05
Street Canyon	0.88	0.96	2.49	1.59	1.92	1.23	-0.79
Open Space	0.93	0.98	2.52	0.74	2.41	1.66	-0.66

### 3.1.2. Globe thermometer measurement results

To test the reliability of recalibrated MRT estimation methods for different sensors, this study applied three globe thermometers to obtain the globe temperature, including 40mm black globe, 40mm grey globe, and 25.4mm black globe (Kestrel). As shown in Fig. 4, globe temperature (Tg) was positively correlated with air temperature and downward shortwave radiation, regardless of thermometer types. In detail, Kestrel globe was more sensitive to the increments of air temperature and shortwave radiation due to its smaller diameter. Grey globe was more sensitive than the black one, which is reported in a previous study measured indoor (Walikewitz et al., 2015).

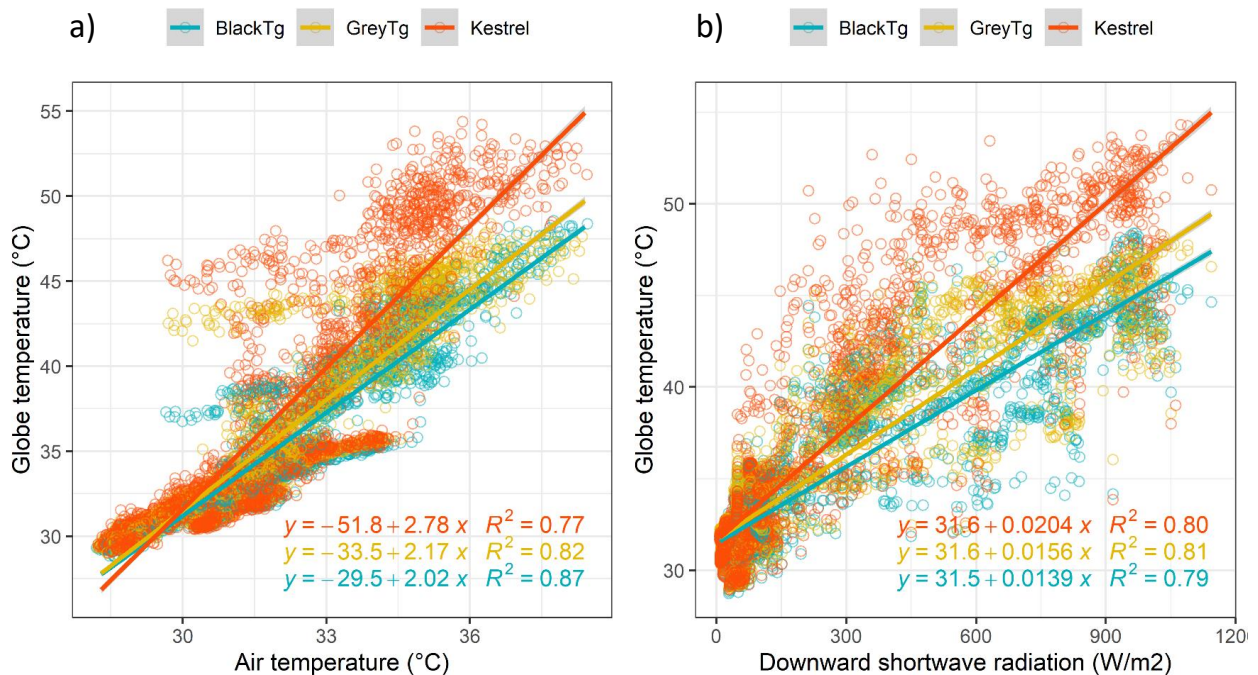


**Fig. 4.** Globe thermometer: a) tg vs. AT by three devices, b) Tg vs. SWdown by three devices

### 3.2. Impacts of time intervals

A previous study found the analysis time interval affects the performance of MRT estimation methods in outdoor environment (Thorsson et al., 2007), while the time interval means taking the average at different time scales. This section investigates the impacts of time intervals, i.e., 1 min, 5min, and 10min, on the performance of the ISO standard method for MRT estimation. As shown in Fig. 5, ISO method at 5min and 10min intervals yielded a better estimation result, as the scattering of the data was narrowed and correlation coefficients were improved significantly. The detailed deviations of MRT by ISO method were listed in Table 4. With increasing time intervals, the estimation biases were decreased:

RMSE was reduced by 1.2 – 1.4 °C at 10min interval in contrast to 1min interval, while MBE was decreased by 0.2 – 0.3 °C.

In addition, larger time intervals effectively removed the abnormally high values of MRT, i.e., MRT above 100 °C was apparently removed by 10min interval. However, at 10min interval, the MRT values by ISO method were still abnormally high compared to the benchmark. This shows the deficiency of the standard method for its application in a subtropical climate background like HK city. Therefore, the recalibration is conducted in the next section.

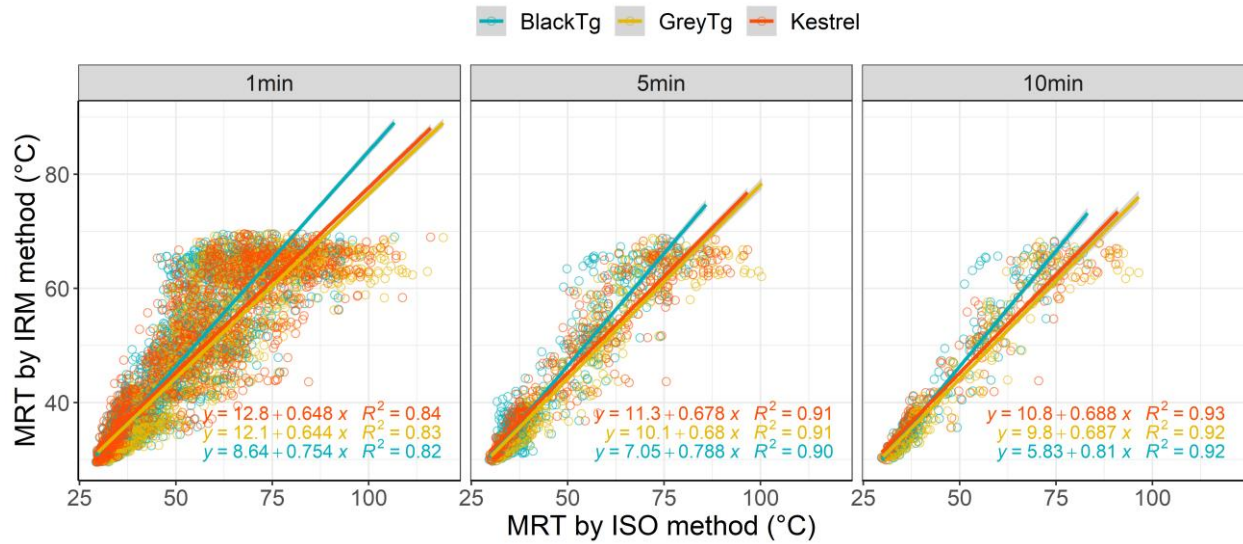


**Fig. 5.** MRT calculated by ISO standard coefficient and MRT measure by integral radiation method

**Table 4.** Quantitative metrics of MRT estimated by Tg (ISO standard method) and by integral radiation method

Time Interval	Device	R <sup>2</sup>	d	RMSE	RMSE <sub>s</sub>	RMSE <sub>u</sub>	MAE	MBE
1min	Black Tg	0.82	0.93	6.67	2.73	6.09	4.25	2.50
	Grey Tg	0.83	0.90	9.20	5.89	7.06	5.63	4.81
	Kestrel	0.84	0.91	8.41	4.89	6.84	4.79	3.40
5min	Black Tg	0.90	0.96	5.51	3.00	4.61	3.80	2.53
	Grey Tg	0.91	0.92	8.27	6.50	5.11	5.30	5.16
	Kestrel	0.91	0.93	7.41	5.50	4.97	4.27	3.66
10min	Black Tg	0.92	0.96	5.06	3.26	3.88	3.41	2.80
	Grey Tg	0.92	0.92	8.04	6.57	4.63	5.22	5.18
	Kestrel	0.93	0.94	7.03	5.57	4.29	4.02	3.65

### 3.3. Recalibrating the convection coefficient

Based on MRT by integral radiation method and microclimate variables, i.e., AT and WS, the convection coefficient of the globe can be recalibrated by non-linear regression. To obtain convection coefficient, equation (3-4) is transformed to be equation (5):

$$a * V_a^b = \frac{(MRT+237.15)^4 - (T_g+273.15)^4}{T_g - T_a} * \epsilon D^4 \quad (5)$$

K-fold cross-validation is a resampling procedure to train, test, and validate the models. By splitting a given dataset into k equally-sized subsets randomly, one subset is used for testing, while the remaining

subsets are used for training. After each subset is used for both training and testing, the iterations are finished and the test errors can be obtained by averaging all models' errors. Usually, it is recommended to use  $k = 5$  or  $10$ , considering both computational advantages and bias-variance trade-off (James et al., 2013). Therefore, this study applied 5-fold cross-validation (80% as training and 20% as testing) to determine the final optimal model, which yields the convection coefficient as  $a = 0.676 \cdot 10^8$ ,  $b = 0.019$  in the outdoor environment of the humid subtropical climate background, considering all measurement locations (open space, street canyon, and under tree) and time intervals (1min, 5min, and 10min). The recalibrated coefficients are valid when wind speed ranging from 0.23 to 3.06 m/s and downward shortwave radiation less than 1036 W/m<sup>2</sup>.

### 3.4. Comparing different recalibrated methods for MRT estimation

#### 3.4.1. Comparing based on error probability of two accuracy requirements

ISO standard 7726:1985 specified the requirements of the accuracy for MRT at different conditions, i.e., the measuring accuracy requirement should be  $\pm 2$  °C for thermal comfort level and  $\pm 5$  °C for thermal stress level (ISO, 1985). To cross-compare different MRT estimation methods for their performance, the error probability was calculated by the percentage of data above the threshold of  $\pm 2$  °C and  $\pm 5$  °C respectively. Shown in **Fig. 6**, the error probability of different methods varied significantly, and the variation was also presented for different measurement locations and devices.

Regarding the differences of measurement locations, a higher error probability was presented at open space than street canyon and under tree locations. In detail, for comfort requirement at  $\pm 2$  °C, in open space, the error probability was high as 76 – 100% (TeitelbaumForce – Tan) for all previous methods. For street canyon location, the error probability was high when applying Tan (89%), VanosBlack (61%), and VanosGrey (61%), with the lowest value for TeitelbaumForce (28%) and TeitelbaumMix (29%). In terms of under tree, high error probability was shown by Tan (96%), Manavvi (59%), and Thorsson (52%), while low values were found for TeitelbaumForce (19%) and TeitelbaumMix (25%). The localized recalibrated method (HKCorrect) outperformed with the error probability of 45%, 18%, and 5% for open space, street canyon, and under tree locations separately. For heat stress requirement at  $\pm 5$  °C, at open space, all previous studies yielded the error probability of 40 – 97% (Teitelbaum Force – Tan). At street canyon, except the Tan (57%), VanosBlack (31%), VanosGrey (26%) methods, most of the previous studies showed the error probability lower than 25%. Under tree shading, only Tan method presented the high error probability as 63%, while TeitelbaumForce and TeitelbaumMix showed zero error probability. The localized recalibrated method (HKCorrect) still performed the best with the error probability of 13%, 5%, and 0% for open space, street canyon, and under tree locations respectively.

In terms of devices, the performance of methods was not identical. For instance, for comfort requirement at  $\pm 2$  °C, grey globe showed the highest error probability among three devices for ISO (64%), Thorsson (78%), Manavvi (79%), TeitelbaymForce (50%), and TeitelbaymMix (57%), but showed the lowest value for VanosBlack (57%). Kestrel yielded the lowest error probability for ISO (39%), Thorsson (48%), Tan (87%), Manavvi (54%), TeitelbaymForce (32%), and TeitelbaymMix (33%). Similarly, for the comfort requirement at  $\pm 5$  °C, grey globe also presented the highest probability for ISO (33%), Thorsson (43%), Manavvi (48%), TeitelbaymForce (24%), and TeitelbaymMix (27%). But the lowest values were attained by Kestrel for Thorsson (31%), Tan (53%), Manavvi (37%), TeitelbaymFree (28%), Acero (16%), while by black globe for ISO (23%), TeitelbaymForce (12%), TeitelbaymMix (15%), VanosBlack (38%), and VanosGrey (35%). Recalibrated method in HK (HKCorrect) showed the best performance among all the methods, which presented the lowest error probability, i.e., 28%, 22%, 18% for black, grey globe and Kestrel at  $\pm 2$  °C requirement, and 13%, 2%, 4% at  $\pm 5$  °C requirement.

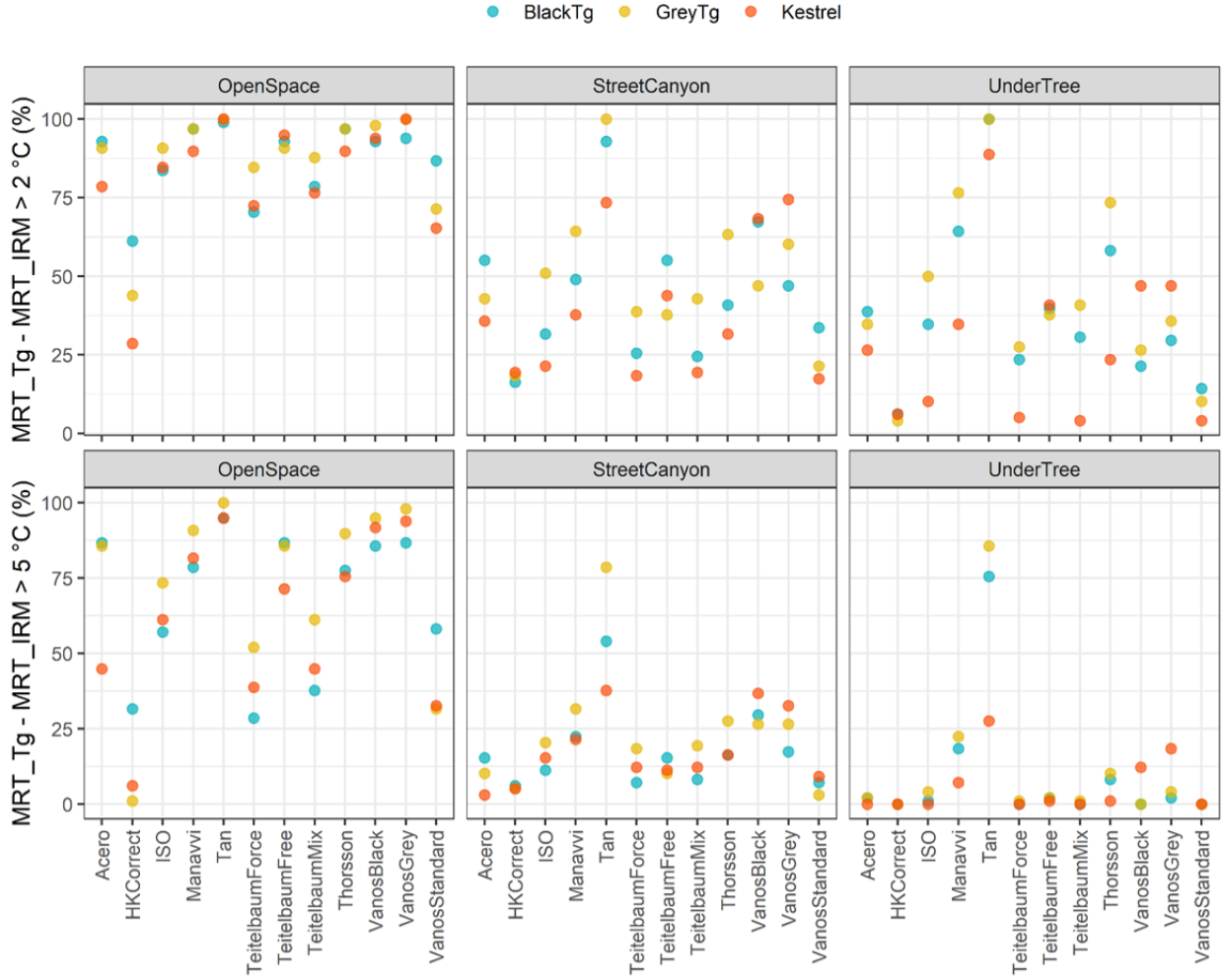


**Fig. 6.** Error probability (bias > 2 °C and 5 °C) at 10 min interval

### 3.4.2. Comparing based on quantitative metrics

The performance of different methods was quantified further by five metrics, shown in **Fig. 7**. Among all recalibrated methods, the localized recalibrated method (HKCorrect) exerted the best performance, with relatively high  $R^2$  and  $d$  ( $R^2 = 0.84$ ,  $d = 0.95$ ), and lowest errors and biases (RMSE = 3.84 °C, MBE = -1.36 °C, MAE = 2.61 °C), while the standard ISO method yielded the results of  $R^2 = 0.84$ ,  $d = 0.92$ , RMSE = 7.91 °C, MBE = 3.63 °C, MAE = 4.77 °C. The metrics for other methods were revealed in **Table 5**.

**Table 5.** Quantitative metrics of different MRT estimation methods

Methods	$R^2$	$d$	RMSE	RMSEs	RMSEu	MAE	MBE
ISO	0.84	0.92	7.91	4.58	6.45	4.77	3.63
Thorsson	0.80	0.86	11.38	7.63	8.44	6.77	5.88
Tan	0.92	0.80	15.86	14.69	5.98	12.07	12.04
Manavvi	0.72	0.79	15.74	10.55	11.69	8.96	7.94
TeitelbaumFree	0.91	0.90	6.41	5.93	2.43	4.46	-4.30
TeitelbaumForce	0.86	0.95	5.96	2.65	5.34	3.65	2.20
TeitelbaumMix	0.86	0.94	6.41	3.26	5.52	3.92	2.67
VanosStandard	0.85	0.96	4.87	1.57	4.61	3.03	-1.00

VanosBlack	0.82	0.78	17.52	13.85	10.73	10.08	8.16
VanosGrey	0.84	0.79	16.84	13.75	9.72	9.97	9.30
Acero	0.87	0.90	6.57	5.84	3.00	4.42	-4.17
<b>HKCorrect</b>	<b>0.84</b>	<b>0.95</b>	<b>3.84</b>	<b>1.97</b>	<b>3.29</b>	<b>2.61</b>	<b>-1.36</b>

Regarding the impacts of the measurement locations on the accuracy of MRT estimation, the two dimensionless metrics  $R^2$  and  $d$  showed more sensitivity to the methods than to the locations. For instance, Manavvi presented the relatively deficient performance ( $R^2 = 0.58 - 0.78$ ,  $d = 0.57 - 0.78$ ) in all locations, while Teitelbaum Force and Teitelbaum Mix methods showed the continuously high values regardless of locations ( $R^2 = 0.75 - 0.85$  and  $0.74 - 0.84$ ,  $d = 0.87 - 0.92$  and  $0.85 - 0.91$  respectively). Besides, Tan presented opposite performance with relatively high  $R^2$  ( $0.74 - 0.84$ ) but moderately low  $d$  ( $0.50 - 0.73$ ) in all locations. As for three metrics quantifying bias and error, the values of open space were much higher than that of street canyon and under tree locations, whose differences were higher than  $10\text{ }^\circ\text{C}$  or even up to  $20\text{ }^\circ\text{C}$ . In details, some recalibrated methods yielded high errors and biases in open spaces, such as Tan method (RMSE =  $24.75\text{ }^\circ\text{C}$ , MBE =  $23.24\text{ }^\circ\text{C}$ , MAE =  $23.24\text{ }^\circ\text{C}$ ), Manavvi (RMSE =  $21.01\text{ }^\circ\text{C}$ , MBE =  $16.28\text{ }^\circ\text{C}$ , MAE =  $16.48\text{ }^\circ\text{C}$ ), Vanos Black (RMSE =  $27.47\text{ }^\circ\text{C}$ , MBE =  $22.47\text{ }^\circ\text{C}$ , MAE =  $22.67\text{ }^\circ\text{C}$ ), and Vanos Grey methods (RMSE =  $26.40\text{ }^\circ\text{C}$ , MBE =  $22.40\text{ }^\circ\text{C}$ , MAE =  $22.45\text{ }^\circ\text{C}$ ). But for street canyon and under tree location, the estimation errors and biases of these methods were reduced apparently, i.e., Tan method (RMSE =  $6.33 - 9.55\text{ }^\circ\text{C}$ , MBE =  $5.90 - 7.27\text{ }^\circ\text{C}$ , MAE =  $5.90 - 7.28\text{ }^\circ\text{C}$ ), Manavvi (RMSE =  $3.64 - 10.15\text{ }^\circ\text{C}$ , MBE =  $2.81 - 5.25\text{ }^\circ\text{C}$ , MAE =  $2.86 - 5.48\text{ }^\circ\text{C}$ ), Vanos Black (RMSE =  $2.39 - 10.19\text{ }^\circ\text{C}$ , MBE =  $0.32 - 2.26\text{ }^\circ\text{C}$ , MAE =  $1.77 - 5.57\text{ }^\circ\text{C}$ ), and Vanos Grey methods (RMSE =  $2.82 - 9.87\text{ }^\circ\text{C}$ , MBE =  $1.56 - 4.69\text{ }^\circ\text{C}$ , MAE =  $2.10 - 5.49\text{ }^\circ\text{C}$ ). This kind of difference can be partly explained by the stronger solar radiation received in the open space. The detailed differences between different locations can be found in **Table A1** in the **Appendix**. Moreover, VanosStandard showed the lowest errors and biases irrespectively of the locations, with RMSE =  $1.20 - 6.20\text{ }^\circ\text{C}$ , MBE =  $-1.87 - -0.33\text{ }^\circ\text{C}$ , MAE =  $0.93 - 4.95\text{ }^\circ\text{C}$ , which can be explained that this method was recalibrated with a standard globe. Thus the impacts of the devices should be explored further.

The results also showed that devices had effects on the accuracy of MRT estimation, as different recalibrated methods showed inconsistent patterns. For instance, the standard ISO method showed lower errors and biases for black globe with RMSE =  $5.06\text{ }^\circ\text{C}$ , MBE =  $2.80\text{ }^\circ\text{C}$ , MAE =  $3.41\text{ }^\circ\text{C}$ , compared with RMSE =  $7.03 - 8.04\text{ }^\circ\text{C}$ , MBE =  $3.65 - 5.18\text{ }^\circ\text{C}$ , MAE =  $4.02 - 5.22\text{ }^\circ\text{C}$  for grey globe and Kestrel. Although Thorsson suggests using grey globe thermometer (Thorsson et al., 2007), the comparison showed that Thorsson method presented lower errors and bias based on black globe than that of grey globe: RMSE =  $7.94$  vs.  $11.77\text{ }^\circ\text{C}$ , MBE =  $5.01$  vs.  $7.74\text{ }^\circ\text{C}$ , MAE =  $5.35$  vs.  $7.75\text{ }^\circ\text{C}$ . In terms of the localized recalibrated method, HKCorrect reached the lowest estimation errors and biases for grey globe (RMSE =  $1.91\text{ }^\circ\text{C}$ , MBE =  $0.28\text{ }^\circ\text{C}$ , MAE =  $1.43\text{ }^\circ\text{C}$ ) than Kestrel and black globe (RMSE =  $2.03 - 3.70\text{ }^\circ\text{C}$ , MBE =  $-1.35 - -0.25\text{ }^\circ\text{C}$ , MAE =  $1.25 - 2.14\text{ }^\circ\text{C}$ ). Other details regarding different devices were reported in **Table A2** in the **Appendix**.



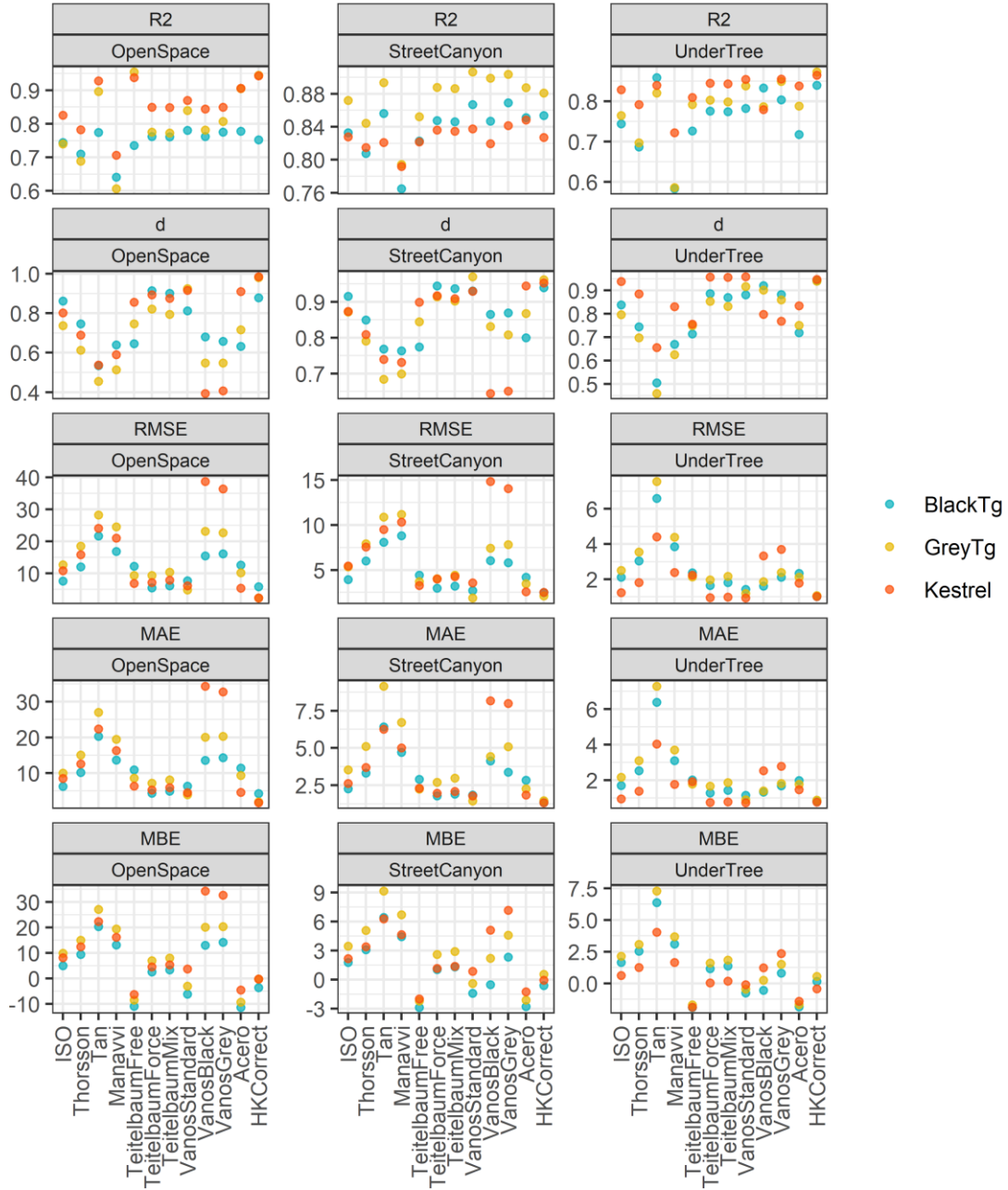


**Fig. 7.** Quantitative metrics of the performance of MRT estimation methods at 10min interval (*Unit of RMSE, MAE and MBE: °C*)

## 4. Discussion

### 4.1. Recalibration and transferability of methods

Previous studies recalibrated the convection coefficients when estimating MRT based on Tg, because the conventional method for MRT estimation is developed for the standard environmental conditions, i.e., low wind speed (< 0.15 m/s) and moderate temperature (= 20 °C) (ISO, 2001), thus they may not be applicable for outdoor environment in different climate backgrounds (Kántor et al., 2015). Summarized in **Table 2**, the recalibrated coefficients are various for different climate types with various wind and solar conditions.

To investigate the transferability of the recalibrated coefficients to other cities, this study cross-compared the performance of different convection coefficients in a subtropical climate background. Three measurement locations and three types of globe thermometers were involved for the comparison. The results showed the recalibrated coefficients performed inconsistently, some coefficients were inferior to others, especially for open space. Besides, even though with similar climate background, the transferability is not definitely feasible. For instance, Singapore is in a similar hot and humid as well as high solar radiation with HK, yet the method developed by Tan (Tan et al., 2013, 2015) was not applicable in HK with high errors and biases (RMSE = 15.86 °C, MBE = 12.04 °C, MAE = 12.07 °C). India is in the same humid subtropical (*Cfa*) climate with HK, the method developed by Manavvi (Manavvi & Rajasekar, 2020) was also with large deviations from the benchmark by the integral radiation method (RMSE = 15.74 °C, MBE = 7.94 °C, MAE = 8.96 °C). Another method conducted in Singapore by Acero (Acero et al., 2021) showed relatively lower errors and biases, but still much above  $\pm 2$  °C (RMSE = 6.57 °C, MBE = -4.17 °C, MAE = 4.42 °C). These results indicate the transferability of the recalibrated methods is limited, which can be partially explained that radiant environment and wind velocity vary largely. Therefore, the results in this study signify the necessity to recalibrate the convection coefficients when estimating MRT with  $T_g$  when the accuracy requirement is high up to  $\pm 2$  °C.

#### 4.2. Recalibration and convection process

There are two types of errors and biases, one is between the globe thermometer and the integral radiation method, another is between the different estimation methods based on the globe thermometer. The former type is partly explained by the shape of the standing men, as the globe thermometer is based on the sphere while the integral radiation method is based on the cuboid shape (Brown, 2019). Besides, the globe thermometer is an indirect way to derive MRT by determining the energy balance of a measuring system, while the integral radiation method is an active method to measure the shortwave and longwave radiant fluxes in six directions to represent a human body (Staiger & Matzarakis, 2020). Therefore, the integral radiation method has been identified to be the most accurate so far for MRT estimation (Thorsson et al., 2007), and used as the benchmark to compare the different calibrated coefficients. As for the errors and biases between the different convection coefficients, there are two possible explanations. One is based on the characteristics of the globe, the emissivity of the globe is varied based on the coating color (ISO, 2001), thus the deviations of black and grey globes are different given the results in this study. Another main reason is the different climate background, i.e., the wind speed and solar radiation conditions, which affect the convection processes of the globe.

The recalibration is emphasized for localized application, since the convection process varies due to the different climate backgrounds. The varying coefficients can be explained by the assumption of the globe thermometer, which refers to the balance of the thermal exchanges between the globe and the microclimate environment (ISO, 2001). This balance is achieved by convection, in which the heat transferring between the air inside the globe and its surrounding environment. There are mainly two types of convection: free convection and forced convection (Teitelbaum et al., 2020). Previous studies indicate that free convection is dominant when the wind speed is low, i.e., lower than 0.2 m/s in (Teitelbaum et al., 2020), while forced convection becomes more importantly with increasing wind speed compared to free convection. This means for outdoor studies using 40mm diameter globe, forced convection plays a dominating role (Vanos et al., 2021). Therefore, mixed convection is suggested to be considered for MRT estimation (Vanos et al., 2021). Our study confirmed this finding by comparing the recalibrated methods based on the free, forced and mixed convection processes, and the results showed when applying in a subtropical climate city, like Hong Kong, the TeitelbaumForce and TeitelbaumMix methods showed slightly higher fits ( $R^2 = 0.86$ ,  $d = 0.94 - 0.95$ ) and slightly lower

biases (RMSE = 5.96 – 6.41 °C, MBE = 2.20 – 2.67 °C, MAE = 3.65 – 3.92 °C) than TeitelbaumFree method ( $R^2 = 0.91$ ,  $d = 0.90$ , RMSE = 6.41 °C, MBE = -4.30 °C, MAE = 4.46 °C).

### **4.3. Impacts of time intervals**

The convection balance of the globe thermometer is also affected by the analysis time intervals, as the outdoor environment is featured with a fast-varying wind and radiative condition. This study compared three time intervals: 1min, 5min, and 10min for their impacts on the MRT estimation. The results in this study were consistent with the findings in the previous study that a larger interval can smooth the deviations of the wind, radiation, and temperature, so that the MRT estimation is more realistic compared to the benchmark (Acero et al., 2021; Teitelbaum et al., 2020; Thorsson et al., 2007). Therefore, 10min time interval is used and suggested in our study when estimating MRT in outdoor environment based on  $T_g$ , which was also recommended by (Marino et al., 2018).

### **4.4. Significance and implications**

This study, to our knowledge, is the first study to systematically compare the MRT estimation methods based on  $T_g$ . It contributes to the urban climate and outdoor thermal comfort studies in two aspects: 1) for studies in a subtropical climate city in HK, this study provides a new recalibrated coefficient for MRT estimation, so that the MRT can be estimated through the cheap and convenient method (globe thermometer) and with relatively high accuracy; 2) for studies in other cities, this study implies that it should be cautious to use ISO standard method to estimate MRT, or directly apply the recalibrated coefficients in different cities, especially when the requirement of the accuracy for MRT is high as  $\pm 2$  °C for thermal comfort level (ISO, 1985).

### **4.5. Limitations and further studies**

The limitations are discussed for a better understanding in this study and for inspiring future studies. Firstly, this study only focused on the typical summer days in Hong Kong, and compared the sites with different SVFs. This is because the heat stress is severe in the summer period as solar radiation is dominant for energy fluxes, and the typical summer day is the most frequent in Hong Kong (Z. Tan et al., 2017). Thus, this study proved that the newly recalibrated coefficients are valid in the summer season in partially cloudy weather conditions. Its feasibility in other meteorological conditions and seasons should be tested in the following studies. Secondly, this study focused on comparing the applicability of different MRT estimation methods and their performance in different sites and by different measurement devices, thus it only covers the three types of urban morphology types, namely open space, street canyon, and under tree. However, there are other morphological characteristics, i.e., building height, building density, and aspect ratio, whose impacts on the convection process of globe thermometer is a possible direction to explore.

## **5. Conclusions**

Mean radiant temperature (MRT), as one of the most significant microclimate variables, has been widely estimated by globe thermometers in outdoor thermal comfort studies. To improve the accuracy of MRT estimation, recalibrated methods have been proposed and applied in different cities. It is worth exploring whether these recalibrated methods can be transferred to other cities. Inspired by this pending question, this study applied MRT by the integral radiation method (also known as six-directional method) as the benchmark, and compared the performance of different recalibrated methods for estimating MRT based on thermometer temperature in a subtropical climate city, Hong Kong. The convection coefficient was recalibrated through non-linear regression analysis for MRT estimation based on  $T_g$ , and joined in the performance comparison. Besides, the impacts of measurement locations, thermometer types, and analysis time intervals were also investigated. The findings of this study can be summarized in the following aspects:

- 1) For the performance of different methods, the ISO standard method and recalibrated methods in different cities should be carefully used in the open space in a subtropical climate. Especially for accuracy requirement at  $\pm 2$  °C, it is suggested to take a local recalibration for the convection coefficient instead of directly using the formula in the literature.
- 2) For different globe thermometers, Kestrel and Grey globe are more recommended in the outdoor environment in the subtropical climate background, as they presented higher fits, lower errors and biases in contrast to the benchmark. Black globe can be applied when the accuracy requirement is  $\pm 5$  °C.
- 3) For analysis time intervals, 1min interval is not recommended when estimating MRT based on Tg in the outdoor environment, as the varying wind and solar conditions may bring many uncertainties for the results. This study suggests applying 10min as the analysis interval, 5min is also appropriate when the wind and solar conditions are stable.

This study indicates that thermometer devices can be used in outdoor environment, but the convection coefficient should be recalibrated carefully. The coefficients in the previous studies may be transferable in the street canyon or tree-shaded areas with an accuracy requirement at  $\pm 5$  °C, but should not be applied in the open space with an accuracy requirement at  $\pm 2$  °C. The findings of this study contribute to improving the MRT measurement accuracy based on cheap methods.

## Acknowledgment

This research is supported by the General Research Fund (RGC Ref No. 14617220) from the Research Grants Council (RGC) of Hong Kong.

## Appendix A

**Table A1.** Quantitative metrics of different MRT estimation methods for three locations at 10 min interval

Location	MRT methods	R <sup>2</sup>	d	RMSE	RMSEs	RMSEu	MAE	MBE
Open Space	ISO	0.74	0.79	10.54	8.09	6.75	8.24	7.70
	Thorsson	0.70	0.67	15.63	13.01	8.66	12.59	12.28
	Tan	0.84	0.50	24.75	23.90	6.46	23.24	23.24
	Manavvi	0.63	0.57	21.01	17.44	11.70	16.48	16.28
	TeitelbaumFree	0.79	0.74	9.67	9.20	2.99	8.61	-8.59
	TeitelbaumForce	0.77	0.87	7.47	4.85	5.67	5.58	4.67
	TeitelbaumMix	0.77	0.85	8.27	5.84	5.87	6.33	5.60
	VanosStandard	0.66	0.89	6.26	2.03	5.92	4.95	-1.87
	VanosBlack	0.64	0.48	27.47	24.07	13.24	22.67	22.47
	VanosGrey	0.67	0.49	26.40	23.65	11.72	22.45	22.40
	Acero	0.69	0.74	9.84	9.02	3.93	8.47	-8.45
	<b>HKCorrect</b>	<b>0.84</b>	<b>0.95</b>	<b>3.84</b>	<b>1.97</b>	<b>3.29</b>	<b>2.61</b>	<b>-1.36</b>
Street Canyon	ISO	0.83	0.88	4.96	3.38	3.63	2.80	2.46
	Thorsson	0.81	0.81	7.21	5.51	4.66	4.04	3.86
	Tan	0.84	0.73	9.55	8.45	4.45	7.28	7.27
	Manavvi	0.78	0.73	10.15	7.96	6.31	5.48	5.25
	TeitelbaumFree	0.80	0.84	3.82	3.45	1.64	2.48	-2.36
	TeitelbaumForce	0.85	0.92	3.70	2.09	3.05	2.15	1.60
	TeitelbaumMix	0.84	0.91	4.00	2.44	3.17	2.32	1.86
	VanosStandard	0.79	0.94	2.80	0.51	2.75	1.69	-0.33

	VanosBlack	0.78	0.74	10.19	7.52	6.88	5.57	2.26	
	VanosGrey	0.81	0.74	9.87	7.87	5.95	5.49	4.69	
	Acero	0.80	0.88	3.48	2.94	1.86	2.31	-2.06	
	<b>HKCorrect</b>	<b>0.83</b>	<b>0.95</b>	<b>2.37</b>	<b>1.04</b>	<b>2.13</b>	<b>1.38</b>	<b>-0.05</b>	
Under Tree	ISO	0.74	0.85	2.03	1.48	1.39	1.61	1.47	
	Thorsson	0.68	0.76	2.90	2.29	1.77	2.35	2.29	
	Tan	0.74	0.52	6.33	5.99	2.04	5.90	5.90	
	Manavvi	0.59	0.69	3.64	2.83	2.29	2.86	2.81	
	TeitelbaumFree	0.77	0.74	2.25	2.13	0.72	1.92	-1.82	
	TeitelbaumForce	0.75	0.90	1.58	0.98	1.23	1.24	0.94	
	TeitelbaumMix	0.74	0.88	1.73	1.15	1.29	1.37	1.13	
	VanosStandard	0.80	0.92	1.20	0.83	0.86	0.93	-0.43	
	VanosBlack	0.75	0.86	2.39	1.19	2.08	1.77	0.32	
	VanosGrey	0.81	0.83	2.82	2.10	1.88	2.10	1.56	
	Acero	0.77	0.77	2.09	1.95	0.75	1.75	-1.64	
		<b>HKCorrect</b>	<b>0.82</b>	<b>0.94</b>	<b>1.04</b>	<b>0.61</b>	<b>0.84</b>	<b>0.83</b>	<b>0.09</b>

**Table A2.** Quantitative metrics of different MRT estimation methods for three devices at 10 min interval

Device	MRT methods	R2	d	RMSE	RMSEs	RMSEu	MAE	MBE
BlackTg	ISO	0.92	0.96	5.06	3.26	3.88	3.41	2.80
	Thorsson	0.91	0.92	7.94	6.19	4.98	5.35	5.01
	Tan	0.94	0.82	13.84	13.01	4.72	11.04	11.04
	Manavvi	0.87	0.87	11.19	8.86	6.82	7.15	6.89
	TeitelbaumFree	0.93	0.85	7.58	7.35	1.86	5.28	-5.24
	TeitelbaumForce	0.93	0.98	3.72	1.65	3.33	2.46	1.56
	TeitelbaumMix	0.93	0.97	4.10	2.22	3.45	2.76	2.02
	VanosStandard	0.94	0.95	4.74	4.21	2.17	3.12	-2.80
	VanosBlack	0.93	0.91	9.61	8.14	5.12	6.35	3.98
	VanosGrey	0.94	0.90	9.95	8.77	4.69	6.46	5.76
	Acero	0.94	0.84	7.78	7.61	1.64	5.43	-5.37
		<b>HKCorrect</b>	<b>0.94</b>	<b>0.97</b>	<b>3.70</b>	<b>2.77</b>	<b>2.44</b>	<b>2.14</b>
GreyTg	ISO	0.92	0.92	8.04	6.57	4.63	5.22	5.18
	Thorsson	0.90	0.86	11.77	10.03	6.16	7.75	7.74
	Tan	0.97	0.76	18.00	17.56	3.94	14.50	14.50
	Manavvi	0.85	0.80	15.77	13.20	8.63	9.97	9.95
	TeitelbaumFree	0.98	0.91	5.91	5.78	1.24	4.21	-4.15
	TeitelbaumForce	0.94	0.95	5.99	4.61	3.82	3.84	3.74
	TeitelbaumMix	0.93	0.94	6.62	5.30	3.96	4.32	4.27
	VanosStandard	0.96	0.98	3.03	2.09	2.19	2.11	-1.32
	VanosBlack	0.94	0.84	14.04	12.84	5.68	8.64	7.51
	VanosGrey	0.95	0.84	13.89	12.95	5.00	9.07	8.80
	Acero	0.97	0.90	6.31	6.17	1.34	4.46	-4.37
		<b>HKCorrect</b>	<b>0.98</b>	<b>0.99</b>	<b>1.91</b>	<b>0.92</b>	<b>1.67</b>	<b>1.43</b>
Kestrel	ISO	0.93	0.94	7.03	5.57	4.29	4.02	3.65
	Thorsson	0.91	0.89	10.15	8.48	5.56	5.88	5.69
	Tan	0.97	0.82	15.12	14.55	4.09	10.88	10.87
	Manavvi	0.88	0.84	13.56	11.21	7.62	7.70	7.49
	TeitelbaumFree	0.97	0.96	4.55	4.24	1.65	3.52	-3.39
	TeitelbaumForce	0.94	0.97	4.71	3.13	3.52	2.67	1.91
	TeitelbaumMix	0.94	0.96	5.18	3.68	3.64	2.94	2.31

VanosStandard	0.95	0.98	4.10	2.56	3.20	2.34	1.49
VanosBlack	0.94	0.71	23.98	22.67	7.82	15.02	13.56
VanosGrey	0.94	0.72	22.59	21.52	6.87	14.51	14.08
Acero	0.96	0.97	3.59	3.00	1.97	2.65	-2.42
<b>HKCorrect</b>	<b>0.97</b>	<b>0.99</b>	<b>2.02</b>	<b>0.26</b>	<b>2.01</b>	<b>1.25</b>	<b>-0.25</b>

## Reference

- Acero, J. A., Dissegna, A., Tan, Y. S., Tan, A., Norford, L. K., Ruefenacht, A., Koh, E. J. Y., Tan, Y. S., & Norford, L. K. (2021). Outdoor Performance of the Black Globe Temperature Sensor on a Hot and Humid Tropical Region. *Environmental Technology*, *0*(ja), 1–20.  
<https://doi.org/10.1080/09593330.2021.1989057>
- ASHRAE. (2001). *2001 ASHRAE Handbook: Fundamentals*. American Society of Heating, Refrigerating and Air-Conditioning Engineers.  
<https://books.google.com.hk/books?id=k9qeAQAACAAJ>
- Brown, R. D. (2019). Correcting the Error in Measuring Radiation Received by a Person: Introducing Cylindrical Radiometers. *Sensors*, *19*(23), 5085. <https://doi.org/10.3390/s19235085>
- Guo, H., Aviv, D., Loyola, M., Teitelbaum, E., Houchois, N., & Meggers, F. (2020). On the understanding of the mean radiant temperature within both the indoor and outdoor environment, a critical review. *Renewable and Sustainable Energy Reviews*, *117*, 109207.  
<https://doi.org/10.1016/j.rser.2019.06.014>
- HKO. (2019). *Summary of Meteorological and Tidal Observations in Hong Kong*.
- HKO. (2020). *Summary of Meteorological and Tidal Observations in Hong Kong*.  
<https://www.hko.gov.hk/tc/publica/smo/files/SMO2020.pdf>
- Höppe, P. (1997). Aspects of human biometeorology in past, present and future. *International Journal of Biometeorology*, *40*(1), 19–23. <https://doi.org/10.1007/BF02439406>
- IPCC. (2021). *Summary for Policymakers. In: Climate Change 2021: The Physical Science Basis. Contribution of Working Group I to the Sixth Assessment Report of the Intergovernmental Panel on Climate Change*.
- ISO. (1985). *BS EN ISO 27726:1994—Thermal environments—Instruments and methods for measuring physical quantities*.
- ISO. (2001). *BS EN ISO 7726:2001—Ergonomics of the thermal environment. Instruments for measuring physical quantities*. <https://www.standardsuk.com/products/BS-EN-ISO-7726-2001>

- James, G., Witten, D., Hastie, T., & Tibshirani, R. (2013). *An introduction to statistical learning* (Vol. 112). Springer.
- Johansson, E., Thorsson, S., Emmanuel, R., & Krüger, E. (2014). Instruments and methods in outdoor thermal comfort studies – The need for standardization. *Urban Climate*, *10*, 346–366.  
<https://doi.org/10.1016/j.uclim.2013.12.002>
- Kántor, N., Kovács, A., & Lin, T.-P. (2015). Looking for simple correction functions between the mean radiant temperature from the “standard black globe” and the “six-directional” techniques in Taiwan. *Theoretical and Applied Climatology*, *121*(1), 99–111.  
<https://doi.org/10.1007/s00704-014-1211-2>
- Kántor, N., & Unger, J. (2011). The most problematic variable in the course of human-biometeorological comfort assessment—The mean radiant temperature. *Central European Journal of Geosciences*, *3*(1), 90–100. <https://doi.org/10.2478/s13533-011-0010-x>
- Kestrel Instruments. (2021). *User guide of Kestrel 5400 Heat Stress Tracker*.  
<https://kestrelinstruments.com/mwdownloads/download/link/id/14/>
- Lai, A., Maing, M., & Ng, E. (2017). Observational studies of mean radiant temperature across different outdoor spaces under shaded conditions in densely built environment. *Building and Environment*, *114*, 397–409. <https://doi.org/10.1016/j.buildenv.2016.12.034>
- Lau, K. K.-L., Lindberg, F., Rayner, D., & Thorsson, S. (2015). The effect of urban geometry on mean radiant temperature under future climate change: A study of three European cities. *International Journal of Biometeorology*, *59*(7), 799–814. <https://doi.org/10.1007/s00484-014-0898-1>
- Lee, H., Jo, S., & Park, S. (2021). A simple technique for the traditional method to estimate mean radiant temperature. *International Journal of Biometeorology*.  
<https://doi.org/10.1007/s00484-021-02213-x>
- Manavvi, S., & Rajasekar, E. (2020). Estimating outdoor mean radiant temperature in a humid subtropical climate. *Building and Environment*, *171*, 106658.  
<https://doi.org/10.1016/j.buildenv.2020.106658>



- Marino, C., Nucara, A., Pietrafesa, M., Polimeni, E., & Costanzo, S. (2018). Outdoor Mean Radiant Temperature Estimation: Is the Black-Globe Thermometer Method a Feasible Course of Action? *2018 IEEE International Conference on Environment and Electrical Engineering and 2018 IEEE Industrial and Commercial Power Systems Europe (EEEIC / I CPS Europe)*, 1–7. <https://doi.org/10.1109/EEEIC.2018.8493714>
- McGregor, G. R. (2012). Human biometeorology. *Progress in Physical Geography: Earth and Environment*, 36(1), 93–109. <https://doi.org/10.1177/0309133311417942>
- Nikolopoulou, M., Baker, N., & Steemers, K. (1999). Improvements to the Globe Thermometer for Outdoor Use. *Architectural Science Review*, 42(1), 27–34. <https://doi.org/10.1080/00038628.1999.9696845>
- Oke, T. R. (1982). The energetic basis of the urban heat island. *Quarterly Journal of the Royal Meteorological Society*, 108(455), 1–24.
- Ouyang, W., Morakinyo, T. E., Ren, C., Liu, S., & Ng, E. (2021). Thermal-irradiant performance of green infrastructure typologies: Field measurement study in a subtropical climate city. *Science of The Total Environment*, 764, 144635. <https://doi.org/10.1016/j.scitotenv.2020.144635>
- Staiger, H., & Matzarakis, A. (2020). Accuracy of Mean Radiant Temperature Derived from Active and Passive Radiometry. *Atmosphere*, 11(8), 805. <https://doi.org/10.3390/atmos11080805>
- Tan, C. L., Wong, N. H., & Jusuf, S. K. (2013). Outdoor mean radiant temperature estimation in the tropical urban environment. *Building and Environment*, 64, 118–129. <https://doi.org/10.1016/j.buildenv.2013.03.012>
- Tan, C. L., Wong, N. H., Tan, P. Y., Jusuf, S. K., & Chiam, Z. Q. (2015). Impact of plant evapotranspiration rate and shrub albedo on temperature reduction in the tropical outdoor environment. *Building and Environment*, 94, 206–217. <https://doi.org/10.1016/j.buildenv.2015.08.001>
- Tan, Z., Lau, K. K.-L., & Ng, E. (2017). Planning strategies for roadside tree planting and outdoor comfort enhancement in subtropical high-density urban areas. *Building and Environment*, 120, 93–109. <https://doi.org/10.1016/j.buildenv.2017.05.017>

- Teitelbaum, E., Chen, K. W., Meggers, F., Guo, H., Houchois, N., Pantelic, J., & Rysanek, A. (2020). Globe thermometer free convection error potentials. *Scientific Reports*, *10*(1), 2652. <https://doi.org/10.1038/s41598-020-59441-1>
- Thorsson, S., Lindberg, F., Eliasson, I., & Holmer, B. (2007). Different methods for estimating the mean radiant temperature in an outdoor urban setting. *International Journal of Climatology*, *27*(14), 1983–1993. <https://doi.org/10.1002/joc.1537>
- Thorsson, S., Rocklöv, J., Konarska, J., Lindberg, F., Holmer, B., Dousset, B., & Rayner, D. (2014). Mean radiant temperature – A predictor of heat related mortality. *Urban Climate*, *10*, 332–345. <https://doi.org/10.1016/j.uclim.2014.01.004>
- Vanos, J. K., Rykaczewski, K., Middel, A., Vecellio, D. J., Brown, R. D., & Gillespie, T. J. (2021). Improved methods for estimating mean radiant temperature in hot and sunny outdoor settings. *International Journal of Biometeorology*, *65*(6), 967–983. <https://doi.org/10.1007/s00484-021-02131-y>
- Walikewitz, N., Jänicke, B., Langner, M., Meier, F., & Endlicher, W. (2015). The difference between the mean radiant temperature and the air temperature within indoor environments: A case study during summer conditions. *Building and Environment*, *84*, 151–161. <https://doi.org/10.1016/j.buildenv.2014.11.004>
- Wang, D., Lau, K. K.-L., Ren, C., Goggins, W. B. I., Shi, Y., Ho, H. C., Lee, T.-C., Lee, L.-S., Woo, J., & Ng, E. (2019). The impact of extremely hot weather events on all-cause mortality in a highly urbanized and densely populated subtropical city: A 10-year time-series study (2006–2015). *Science of The Total Environment*, *690*, 923–931. <https://doi.org/10.1016/j.scitotenv.2019.07.039>
- Wang, S., & Li, Y. (2015). Suitability of acrylic and copper globe thermometers for diurnal outdoor settings. *Building and Environment*, *89*, 279–294. <https://doi.org/10.1016/j.buildenv.2015.03.002>
- Willmott, C. J. (1981). On the Validation of Models. *Physical Geography*, *2*(2), 184–194. <https://doi.org/10.1080/02723646.1981.10642213>

Willmott, C. J. (1982). Some Comments on the Evaluation of Model Performance. *Bulletin of the American Meteorological Society*, 63(11), 1309–1313. [https://doi.org/10.1175/1520-0477\(1982\)063<1309:SCOTEO>2.0.CO;2](https://doi.org/10.1175/1520-0477(1982)063<1309:SCOTEO>2.0.CO;2)